Engineering Failure Analysis 163 (2024) 108539

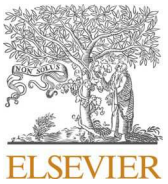

Contents lists available at ScienceDirect

Engineering Failure Analysis

journal homepage: www.elsevier.com/locate/engfailanal

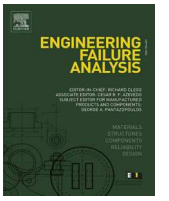

Assessing the behavior of historic masonry buildings to tornadic events: A comparative study of code-based analysis and point cloud based simulation

Saanchi S. Kaushal [a], Mariantonieta Gutierrez Soto [b], Rebecca Napolitano [a,*]

[a] Architectural Engineering Department, Penn State University, US
[b] School of Engineering Design and Innovation, Penn State University, US

ARTICLE INFO

Keywords:
Tornado Damage
Masonry Buildings
ASCE 7–22
Historic Buildings
Finite Element Modeling
Point Cloud

ABSTRACT

During the Midwest Tornado outbreak in December 2021, the historic downtown of Mayfield, Kentucky was heavily impacted. Employing digital documentation, numerical analysis, and on-site wind speed estimations, this study evaluates the behavior of the impacted historic masonry buildings. It explores the structural damages and stress distributions observed in historic masonry buildings impacted by tornadoes, comparing them to predictions made by the ASCE 7–22 standard for tornado loads. Through this investigation, it becomes evident that the stress distribution and damages produced by the on-site tornado wind speeds were significantly different than those derived from the ASCE 7–22 standard. The current standard does not account for most historic structures, typically classified as Risk Category.

II. Based on the results of this research, even when these structures are treated as Risk Category III, the stresses estimated by the standard are much lower than the ones experienced on-site. This disparity raises critical questions for preservationists evaluating similar masonry structures in tornado-prone regions. Historic preservation emphasizes minimal intervention, so understanding and addressing the specific vulnerabilities of historic masonry structures to tornadoes is crucial. The analysis in this study identified uplift forces on the roof and high stresses on windward walls as primary causes of damage in these structures, which aligned with the observed collapse mechanisms. Preservationists can use these insights to develop targeted retrofitting strategies that address these vulnerabilities while minimizing impact on the historic fabric. Recognizing these nuances and their impact on structural behavior is crucial for safeguarding the resilience and significance of historic civil structures. Thus, this study lays the groundwork for developing evidence-based, preservation-sensitive guidelines for mitigating tornado damage to irreplaceable historic masonry structures.

1. Introduction

The devastating impact of tornadoes on the built environment has been a long-standing concern, with the United States alone experiencing almost a thousand tornadoes each year [14]. Despite the low probability of occurrence, these extreme events can cause extensive damage in minutes, leaving little time for evacuation [67]. In the last decade, tornadoes like Joplin, Tuscaloosa, and Moore

* Corresponding author.
E-mail address: nap@psu.edu (R. Napolitano).

https://doi.org/10.1016/j.engfailanal.2024.108539
Received 9 April 2024; Received in revised form 19 May 2024; Accepted 7 June 2024
Available online 18 June 2024

have caused extensive damage and fatalities in their aftermath [39]. Even with recurrent devastating tornado outbreaks, only recently has the ASCE 7-22 standard incorporated tornado loading into its documentation, specifically for Risk Category III and IV structures [5] which include buildings with high occupancy and essential facilities.

Tornadoes are classified between EF0 to EF5 (Enhanced Fujita Scale) based on the damages observed after the event [48]. Even with the turbulent nature of these wind events, only a limited section of the impacted area encounters the high wind speeds associated with the tornado classifications. Tornadoes such as Joplin catalyzed studies to determine tornado characteristics such as speed, flow patterns, pressure variations, and induced forces [58]. One of the primary approaches implemented to estimate these properties relies on the use of tornado simulators in laboratories [27,75], but due to the limited number of simulators these can also be estimated via wind tunnel tests [38]. In the last decade, numerical simulations studies have used large eddy models for wind simulation [38,37] or combined computational fluid dynamic models with a finite element mesh to study tornado-structure interaction [78].

In addition, most of the tornado studies have been focused on wooden and/or residential structures [65,69,42,71]. While researchers have evaluated the behavior of extreme wind loading conditions on low-rise structures and highlighted their increased susceptibility to damage [16,26], they rarely focus on masonry structures. Most masonry construction in the United States dates back to the early 19th century [59], making them an integral part of the built environment. To the authors' knowledge, the investigation conducted by Sparks et al. [68] following the 1984 wind storms (tornado and hurricane) stands as the earliest reference indicating the vulnerability of masonry structures to significant damage, highlighting the necessity for further exploration in this area.

Reconnaissance missions undertaken after multiple tornadoes have documented the damage observed in the masonry structures [46,43,76,57,44]. This work seeks to understand "How do the actual structural damages and stress distributions in historic masonry buildings impacted by tornadoes compare to those predicted by the current ASCE 7-22 standard for tornado loads?". While addressing this question, it also explores the resulting implications for the assessment, strengthening, and preservation of these structures. With tornado loads recently integrated into the design standard, the novelty of the work presented lies in its comprehensive assessment and comparison of the actual structural damages and stress distributions in historic masonry buildings impacted by tornadoes against those predicted by the ASCE 7-22 standard for tornado loads. Employing digital documentation techniques, numerical analysis, and on-site wind speed estimations, this study uniquely assesses the behavior of historic masonry buildings during the December 2021 Midwest Tornado outbreak, with a specific focus on Mayfield, Kentucky's historic downtown. Its methodological approach, direct comparison between observed and predicted structural behaviors under tornado loads, and implications for the preservation and reinforcement of historic masonry structures contribute to the novelty of this work.

1.1. Disaster overview

In December 2021, the unexpected tornado outbreak in the Midwest regions of the United States generated multiple tornadoes [25]. Among these, the Midwest Tornado covered a distance of 250 miles and was categorized as an EF-4 tornado [56]. It passed through Arkansas, Missouri, Tennessee, and Kentucky, leaving behind a trail of destruction, with Kentucky (KY) being the most impacted [66].

In response to this disaster, a two-phased reconnaissance mission was organized to collect damage data from the impacted sites. The first phase was conducted as a part of the Structural Extreme Events Network (StEER) and concentrated on evaluating the widespread damage in the impacted regions in December 2021 [57]. The second phase, organized in March 2022, focused on digitally documenting the historic masonry structures in Mayfield, KY [33].

Mayfield, KY, is a town whose historic downtown was listed in the National Register of Historic Places [54]. The town was established in 1821 and served as a social and economic hub for many years. In 1984, Mayfield's downtown area earned a spot on the National Register of Historic Places due to its diverse architectural styles, evidence of town planning, and significant historical events.

Fig. 1. The original post office (orange) and the additions done in 1950.

Subsequently, the registration was updated in 1995 to include surrounding buildings that also contribute to the town's historic characteristics [55].

In March 2022, the authors conducted a reconnaissance expedition in collaboration with field experts from the RAPID facility at the University of Washington. The primary objective of this mission was to digitally record the historical masonry structures in Mayfield, Kentucky, which had suffered significant damage during the Midwest Tornadoes in December 2021. Since the initial damage assessment conducted in December 2021, many of the impacted historic buildings had been demolished by the time of the reconnaissance in March 2022. Consequently, only 13 historic masonry buildings remained available for documentation. For the current study, the focus lies on the documentation of the US Post Office.

1.2. Case Study: US Post Office

The US Post Office in Mayfield was constructed in 1910, as a replacement to its predecessor, a wooden-framed structure, and features a classical revival style with marbled columns on its entryway and a detailed stone and brick parapet [54]. Even though the building had undergone alterations around the 1950 s, it still retained some of its original features as seen in Fig. 1.

In December 2021, the Midwest Tornado passed close to the US Post Office, according to the estimated path (Fig. 3). This resulted in significant damage to the Post Office, while its adjacent structures were razed to the ground. The damages observed for the Post Office included roof damages, broken windows and wall collapse (Fig. 2).

2. Numerical modeling strategy

The numerical modelling strategy adopted in this study is a result of the data obtained during the March reconnaissance mission. Digital documentation techniques, such as Terrestrial Laser Scanning or Photogrammetry, often serve as the base for generating finite element models [17,20]. This research implements a numerical strategy that provides an efficient means to convert digitally documented structures into finite element models, requiring minimal time intervention. This method consists of two main steps: first, generating the point clouds from the data collected and second, converting these point clouds into finite element models that work with commercial finite element software.

Subsequently, for determining tornado wind speeds and their corresponding loads, this study employs two approaches. The on-site wind speed estimation relied on analyzing tree fall patterns to deduce wind characteristics, offering valuable insights into the tornado's behaviour. The second set of wind speeds were calculated using the ASCE7-22 design standards. Once wind speeds are determined, they were translated into tornado-induced loads through procedures outlined in the ASCE 7–22 standard, as explained in detail ahead.

2.1. Photogrammetric data acquisition and processing

Spatial documentation of a structure often relies on combining photogrammetry and Light Detection and Ranging (LiDAR) techniques. While LiDAR is widely acknowledged for its high precision [49], the combination of both these techniques yields even more accurate results [6]. With that in mind, the US Post Office was documented using both these approaches. The Leica RTC360 LiDAR scanner was employed to capture the external facade of the structure. This choice was predicated on the scanner's capabilities to accurately capture image data at a rate of 2 million points per second, generate a point cloud in under two minutes, and ease of portability [11]. The scanner was positioned at all the corners and mid-points of the structure, totaling to eight scans of the Post Office [33].

In addition, an Unmanned Aerial Vehicle was utilized to capture aerial imagery of the Post Office. For this, the DJI Matrice was flown in a grid-like and circular pattern to maximize images captured of the building. While both the data capture methods are effective, it is evident from Fig. 4 that certain portions of the USPS were not fully covered. This limitation was particularly notable on the roof and walls, where factors such as reflections from stagnant water or limitations in UAV image capture contributed to the gaps in

(a) Wall and Roof Damage **(b)** Broken Windows

Fig. 2. Some of the damages seen on the US Post Office.

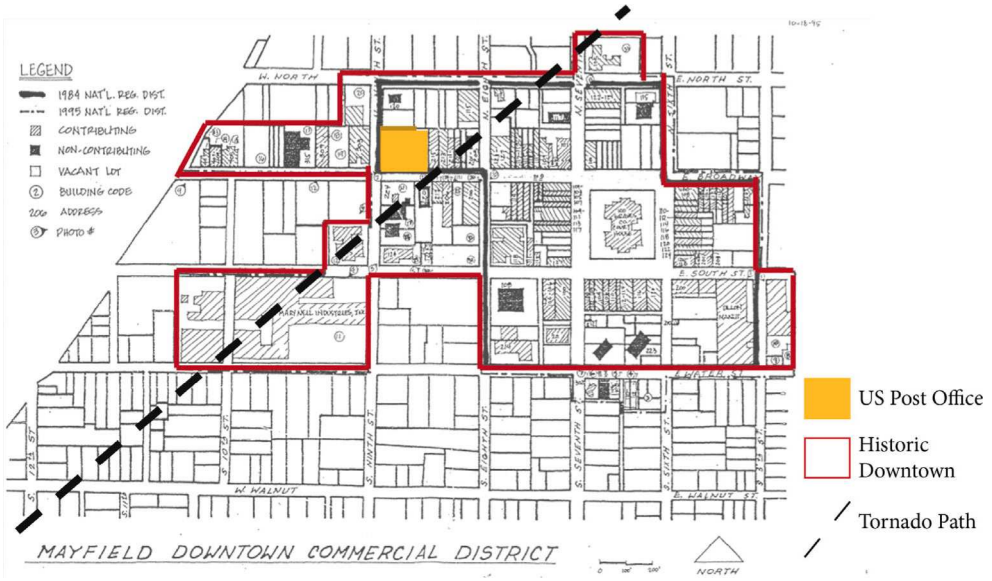

Fig. 3. An overview of the disaster and building location (Mayfield Plan [55]).

data. Therefore, the integration of point clouds from both the UAV and LiDAR played a crucial role in mitigating these "missing" sections of the point cloud. Fig. 5 illustrates the point cloud obtained from combining both data sets.

Following the data capture, the data was processed using a three-step approach. The first two steps concentrated on generating point clouds according to the instrument employed for data capture, while the third step was designed to merge both the point clouds. The UAV images were processed through Pix4D, a widely adopted photogrammetry software known for its point cloud generation capabilities [7]. For the LiDAR scans, the data was imported into Register 360, utilizing its built-in visual alignment tool to align the scans. The primary objective was to achieve a minimum of 90 % overlap between the various scans. The Cyclone package was used to integrate the independently processed point clouds. For more information about the data processing steps, the reader may refer to Kaushal et al [33].

Fig. 4. The point cloud generated for the US Post Office, using the UAV images.

Fig. 5. The final point cloud generated by combining the LiDAR and UAV point clouds.

2.2. Generating the finite element model

The use of point clouds to generate numerical models is an increasingly popular research area. This approach allows creation of highly detailed 3D models [9], which can be used for structural analysis [64], damage assessment [77] and preservation of historic buildings [36]. However, there is an intermediate step which often involves the use of Computer-Aided Design (CAD) to create a geometric replica of the point cloud prior to being used as a numerical model, which is a time-consuming process [17]. In an attempt to reduce the time and effort to produce CAD models, researchers have proposed ways to bypass this step and convert point clouds into a numerically usable model [28,8,18].

Considering the previously mentioned fact, this project employed an open-source software named *Cloud2FEM* for transforming the point clouds into finite element meshes. This software, developed by Castellazzi et al [18], has been validated for various structures and their damages [32,21]. In this software, the point cloud is first sliced vertically into 'n' number of slices, as defined by the user. For

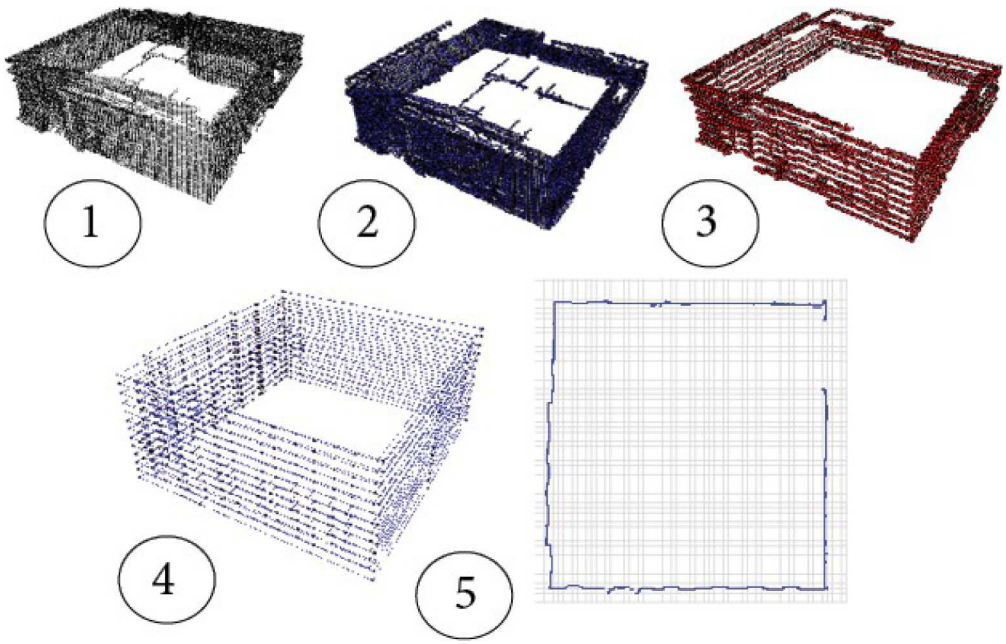

Fig. 6. The steps for generating the finite element mesh in Cloud2FEM.

each of these slices, a closed polygon is created by connecting all the points within it. The closed polygons are usually representative of the internal and external walls. These closed polygons for 'n' slices are then stacked together to generate a 3D voxelized object, where each voxel is converted into an 8-node hexahedral element to form a 3D solid mesh. More details about this process and the software can be found in these references [17,18].

While constructing the mesh for the Post Office (Fig. 6), after inputting the point cloud into Cloud2FEM (Step 1), the point cloud was divided into 52 discrete slices (Step 2). The number of slices was decided based on the preliminary simulations and the height of the structure. Following the generation of slices, centroids were computed for each of these slices (Step 3). It is advisable to eliminate random points and outliers from each slice before centroid computation, as failing to do so resulted in a substantial increase in the computation time. Subsequently, the polylines were formed by connecting adjacent centroids to each other (Step 4). The most time-consuming step is the process of refining these polylines to align with the underlying geometry of the slices point cloud. Once the polyline refinement step is completed, polygons are constructed and meshed (Step 5). It is important to note that the mesh resolution depends on the thickness of the slice, the number of slices and the grid parameters that can be specified in the software's graphical interface.

2.3. On-site wind speed estimation

Estimating the wind speeds in the aftermath of a tornadic event is often a time-consuming task. Research has identified indicators that have previously been used for this estimation, which range from physical damages to residences [40], tree fall patterns [10] to impacted traffic signs [13,61]. Over the years, damages to trees and their fall pattern have been used more broadly to estimate the wind speeds [62].

Following the tornado in Mayfield, 337 trees were identified near downtown to help estimate the wind speed [60]. The authors used these patterns to calculate the parameters for the Rankine Vortex (RV) model to reconstruct the wind field map, offering an independent avenue for wind speed estimation alongside radar measurements and structural damage evaluation. Based on these calculations, the wind speed time history for the Mayfield Post Office was estimated with the peak wind speed as 88 m/s, estimated within a 95 % confidence interval.

2.4. ASCE wind speed estimation

In the updated design standard ASCE 7-22, the chapter (chapter 32) on tornado loads provides probabilistic wind speed maps to estimate these speeds based on parameters such as building area and mean return periods. In evaluating tornadic events between 1995 and 2016, it was observed that lower-intensity tornadoes (EF0, EF1, and EF2) were highly prevalent, accounting for nearly 99 % of all recorded tornadoes [73]. Given this, the current standard provides wind speeds for EF0-EF2 tornadoes for a 1,700 and 3,000-year return period. Notably, ASCE7-22 specifically addresses tornado wind speeds for Risk Category III and IV structures, which encompass critical infrastructure and essential facilities. However, this standard does not provide provisions for historic buildings, typically classified as Risk Category II structures.

Although the tornado wind speeds experienced in Mayfield were estimated to be significantly higher than those prescribed in the code, they were calculated to provide a comparison to the on-site damage observations. These wind speeds are also available for specific locations via an online ASCE Hazard Tool [1], which provides them for return periods between 1,700 to 10,000,000 based on the built area. For the post office building, which had an estimated area of 795 square meters, the wind speed calculated through linear interpolation was 35.4 m/s for a Risk Category III structure, considering the specified return period. However, when assuming the maximum return period of 10,000,000 years, the calculated wind speed for the post office was 114.8 m/s, which is closer to the wind speed estimated through on-site damage analysis.

2.5. Wind load calculation

Once the wind speeds are determined, the wind speeds can be converted into tornado-induced loads by following the procedures outlined in the ASCE 7–22 standard, specifically detailed in Chapter 32 [5]. The calculation of pressure acting on the primary wind force-resisting system (MWFRS) is based on the following equation:

$$p = q \times G_T \times K_d T \times K_V T \times C_p - q_i\left(GC_p i\right) \tag{1}$$

where q is tornado velocity pressure at a specific height of the structure, G_T is the gust factor taken as 0.85, K_{dT} is the directionality factor taken as 0.8, and K_{vT} is the tornado exposure coefficient, assumed to be 1.1. The external pressure coefficient is C_p and the internal pressure coefficient, GC_{pi} results from the multiplication of the gust factor and the internal pressure coefficient. The tornado velocity pressure is computed as:

$$q = 0.613 \times K_z T \times K_e \times V_T \times K_e \times V_T^2 \left[N/m^2\right] \tag{2}$$

where *Ke* is the ground elevation factor and is taken as 1 for a building shorter than 61 m, and *VT*, the design tornado wind speed (m/s). Since the focus of this study is the MWFRS, the components and cladding portions of the tornado load calculation is not included in this paper.

3. Simulation and analysis

To assess the vulnerability of the Post Office under varied tornadic loading, computational simulations were carried out to test the modeling strategy and compare it to the damage on site. The goal was twofold (i) to evaluate the numerical model by comparing the results of the structural analysis to the damages captured on-site, and (ii) to conduct a qualitative assessment of the disparities in damage patterns between the wind speeds estimated on-site and those stipulated by the ASCE 7-22 standard. All numerical modeling and analyses were executed using ABAQUS, a commercial finite element software [2].

Over the last few years, nonlinear analysis has become popular due to the increasing computational power of the available software [63]. During this analysis, the model is loaded incrementally to reach its peak and post-peak stage. At each step, the nonlinear differential equations are solved keeping in mind the model's mechanical nonlinearity [23]. Historical applications of nonlinear static analysis simulations have ranged from gaining insights into the behavior of a historic masonry tower [15] to assessing the damages observed in the aftermath of the 2012 Emilia Earthquake [22]. Given that the goal of this study was to understand how actual structural damages and stress distribution in historic masonry buildings impacted by the tornado compare to those predicted by the current 7-22 standard, the execution of a nonlinear static analysis was a feasible approach. The loading conditions were determined for the main wind force-resisting system and the roof using the wind speeds mentioned earlier.

For the simulations, the tornado pressures were calculated individually for all the walls and the roof. These pressures were then multiplied with the respective surface areas to convert them into uniform loads. Given that these pressures acted at a defined angle on the walls, these were segregated into parallel and perpendicular loading conditions for easier application within ABAQUS.

3.1. Constitutive model

For modeling the nonlinear behavior of masonry, the Concrete Damage Plasticity (CDP) model within ABAQUS was implemented (Table 1). Even though this model was initially developed for brittle materials like concrete [41], it has been extensively used to simulate the behavior of masonry buildings [3,19,74,34]. The model uses concepts of varying material properties in compression and tension, with distinct damage parameters where the main failure mechanisms are tensile cracking and compressive crushing. In tension, the material behaves linearly till the peak stress is reached (σ_t), after which cracks begin to appear. Similarly, in compression, once the material reaches yield stress (σ_c), compression crushing occurs. The damage parameters in tension (d_t) and compression (d_c) are calculated as:

$$\sigma_t = (1 - d_t) \times E_0 \times \left(\in_t - \in_t^{pl}\right) \tag{3}$$

$$\sigma_c = (1 - d_c) \times E_0 \times \left(\in_c - \in_c^{pl}\right) \tag{4}$$

where, σ_t and σ_c are the compressive and tensile stresses, E_0 is the initial elastic modulus, $\in_t$ and $\in_c$ are the total strains, $\in^{pl}$ and $\in^{pl}$ are the plastic strains in tension and compression. The damage parameters have values ranging from 0 (no degradation) to 1 (full degradation).

While implementing this constitutive model in ABAQUS, other parameters like the dilation angle (ψ), eccentricity ($\in$), the ratio between biaxial compressive strength and uniaxial compressive strength ($f\,b0/\,fc$), and a viscosity parameter (χ) are also needed. The dilatancy angle usually varies between 0° to 36°, to capture model behaviour [4], the eccentricity and $f\,b0/\,fc$ values recommended by ABAQUS are 0.1 and 1.16 respectively [2].

3.2. Model calibration and validation

The initial construction material used for the Post Office was was brick masonry. However, when it was renovated, the additional sections were built using concrete masonry units. In the absence of direct experimental data to accurately define the material properties of the Post Office, especially considering that its construction phases involved both brick and concrete masonry units, the approach necessitated a strategy to estimate these properties as accurately as possible. While there was a basic understanding of the potential range of parameters based on existing literature [24,17], the wind speeds [60], and the final damage state of the building after the tornado, these elements alone were insufficient for precise modeling. Consequently, an extensive series of simulations were run, employing an established methodology for parameter estimation of masonry based on observed damages [53]. The need for a robust method to manage and quantify the uncertainties associated with the estimated material properties led to the adoption of the

Table 1
Value of the CDP parameters adopted for the simulation.

Parameter	Value
Dilatancy Angle	20°
Eccentricity	0.1
$f\,b_0/\,fc$	1.16
K_c	0.66
Viscosity Parameter	0.002

Latin Hypercube Sampling (LHS) technique.

LHS was chosen for its efficiency and effectiveness in enhancing the predictive accuracy and reliability of the computational model under these uncertain con– ditions. Unlike conventional random sampling methods, which might overlook certain areas of the parameter space or over-represent others, LHS ensured a comprehensive and even exploration of all possible values of the material properties. By dividing the range of each parameter into intervals of equal probability and randomly selecting a single value from each interval, LHS minimizes sampling bias and maximizes the diversity of the sample set. This approach is particularly valuable in this context, where the accurate representation of material properties is crucial for the reliability of the model's predictions regarding the structural behavior of the building under tornado loads. This iterative process, involving over 200 simulations, was crucial for narrowing down the vast parameter space to identify the set of material properties that most closely mirrored the real-world damage. Each simulation acted as a hypothesis test, with the resulting damage state compared against the empirical evidence. The simulation that resulted in a damage state most akin to what was observed in reality was then selected as representing the most likely material properties of the US Post Office for the purposes of our subsequent analysis. This simulation-based approach allowed the authors to address the challenges posed by the lack of direct material property data, providing a foundation for more accurate and reliable structural analysis. The range of material properties provided to the LHS model was determined based on the masonry quality index [12] and data from Emami et al [52], covering the wide spectrum of possibilities. After running the LHS simulations, the final material properties adopted were from Emami et al [52], since they provided material deterioration values whose results matched well with the on-site damage locations.

To run the simulations, the eastern wall was assumed as the windward wall (Fig. 3), based on the approximate path of the tornado. This assumption was backed by the fact that maximum damage to the structure was observed on this wall and the on-site wind speed angle that was estimated. The primary areas of damage to the Post Office were concentrated on the eastern (windward) wall, the roof, and the windows. These included broken windows and wall collapses, which closely resembled the damages witnessed during the tornado event. Masonry walls are susceptible to damage when subjected to high internal pressures, occurring during the breach of windows and doors, or as a result of combined positive and negative pressures leading to wall collapse [43], as observed for the Post Office (Fig. 7).

Since the focus of this research lies in qualitative assessment of the damages seen, Fig. 8 illustrates the depicts stress patterns and their localized concentrations resulting from uplift forces on the roof, a phenomenon that is very common during tornadic activity. These stress concentration patterns were located near the windows for the Post Office, and can be extrapolated to correlate to roof failures, which often corresponds to the presence of dominant openings including broken windows and doors [51]. The tornado pressures acting on the surface of a structure are spatially heterogeneous and depend on the configuration of the structure, the wind speed and direction, along with the surrounding environment [70], often they are simplified during numerical simulation. The higher turbulent intensities felt at lower heights and the variations in roof loading due to the geometry are the two reasons why tornado impact on low-rise structures can be more complicated [29]. This leads to wall collapses or roofs being torn off [31], which are often preceded by cladding or small-component level failures due to internal pressurization or connection failures due to inappropriate load paths [35].

Furthermore, the authors investigated the variation in stress levels for the simulated model under different enclosure classifications outlined in ASCE7-22. This exploration aimed to comprehend how the structural behavior might differ based on these specifications. Enclosure classifications are crucial in determining internal pressure coefficients utilized for calculating tornadic loads, as per design

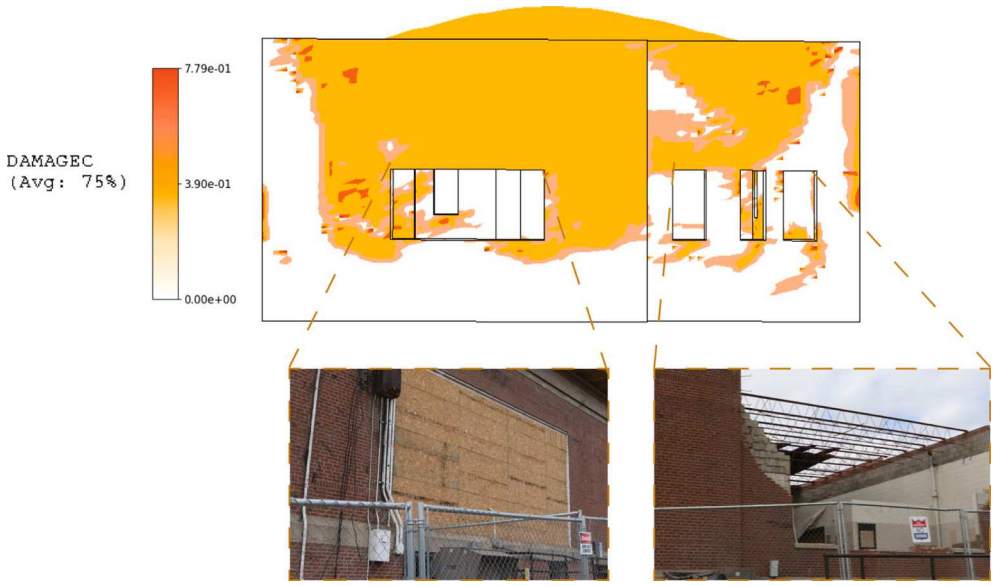

Fig. 7. Comparison between the nonlinear static analysis and the damage seen on-site.

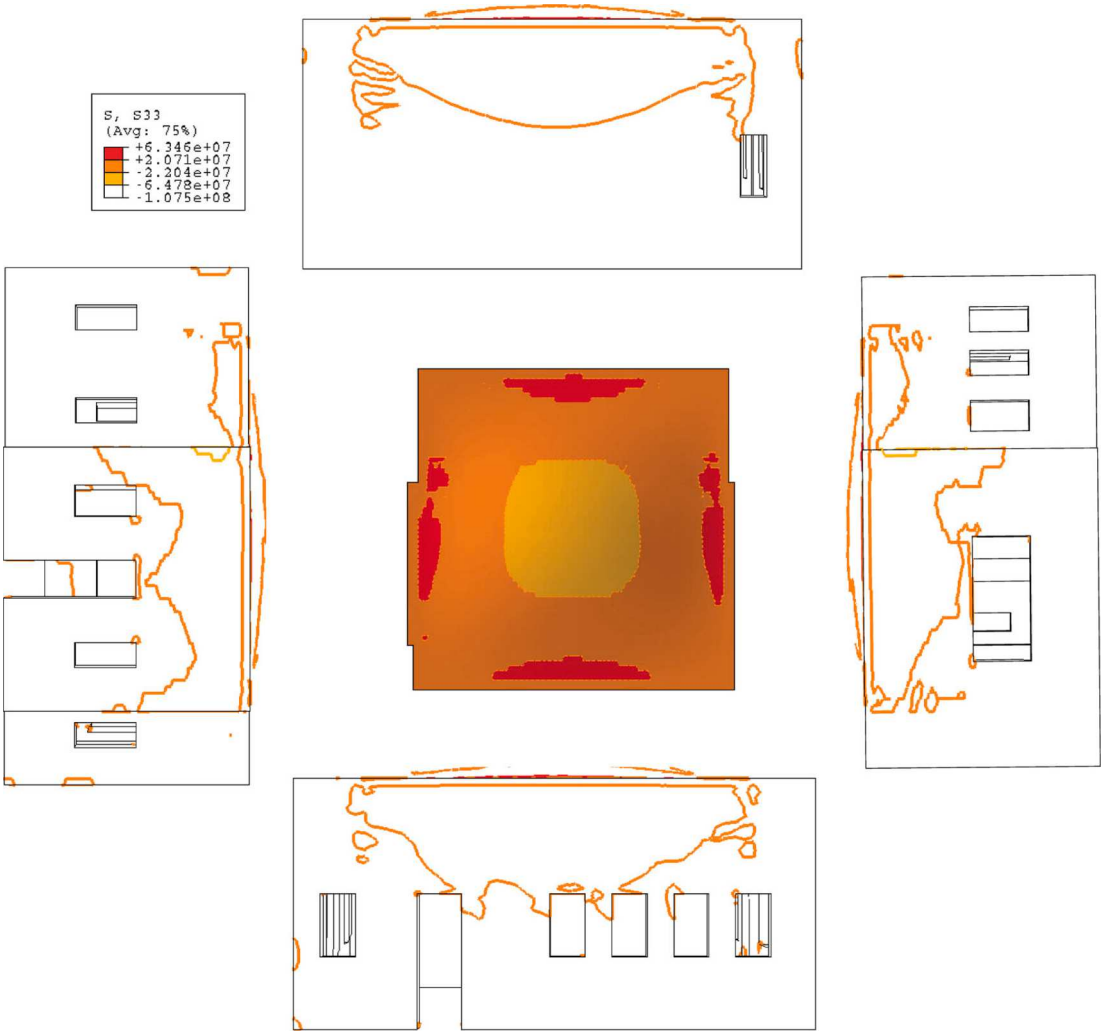

Fig. 8. Stresses generated due to the uplift forces for all the walls.

standards. These classifications are enclosed, open, and partially enclosed structures with high or moderate internal pressure, that vary based on the extent of the openings in the building envelope. Once there's a breach in the structural system, like damaged doors or windows, it's reasonable to consider a partially enclosed condition to exist. Fig. 9 depicts the variation in the total pressure exerted on the walls and roof when the structure was simulated using different enclosure classifications. Regardless of whether it's a wall or the roof that's affected, enclosed structures consistently experience higher pressure levels as compared to other enclosures, while open structures encountered much lower pressures. Even though open structures inherently face lower levels of pressure, when there is a breach in an enclosed structure the sudden escalation in the pressure leads to damage [30]. However, the global behaviour of the structure and the damages incurred will depend on the configuration of the openings [50,72], highlighting the importance of individually identifying the building's requirements to mitigate tornado damage.

3.3. ASCE wind speed based simulations

Following the validation of the model's behavior to match the observed damages on-site, a subsequent round of simulations was conducted, exposing the model to tornado loads corresponding to the ASCE wind speeds. These ASCE wind simulations (L1) were compared to the simulations performed using the on-site wind loads (L2). Prior to the simulations, a comparison of wall and roof pressures between the two wind speeds was conducted, as illustrated in Fig. 10. The comparison revealed that the ASCE stresses were significantly lower in contrast to those encountered by the structure during the tornado, suggesting a greater propensity for extensive damage during a tornado.

Fig. 11 provides a visual representation of the comparative analysis between the stresses produced by the two loading conditions. An examination of the ASCE 7 (L1) loading conditions in comparison to the documented on-site damage reveals that the stress generated were insufficient to induce the uplift or wall damage observed in the field. In contrast, the on-site (L2) loading condition

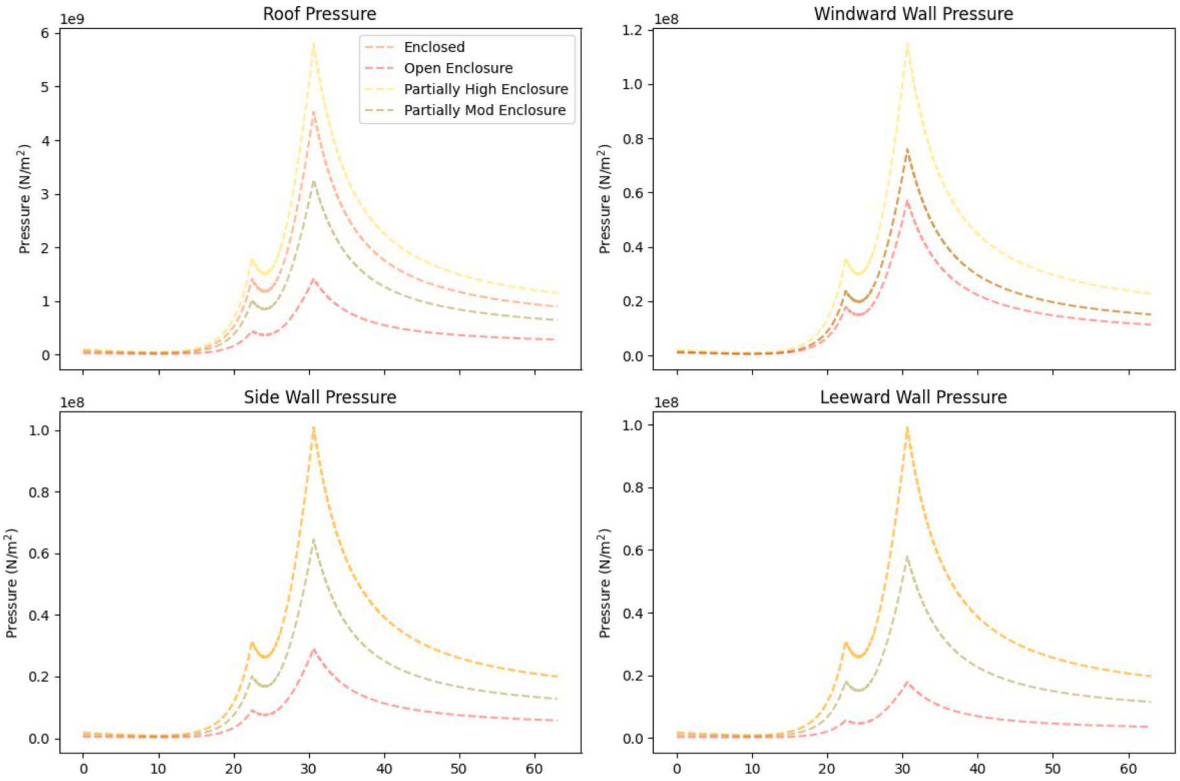

Fig. 9. The pressure variations for all the walls when subjected to on-site loading conditions.

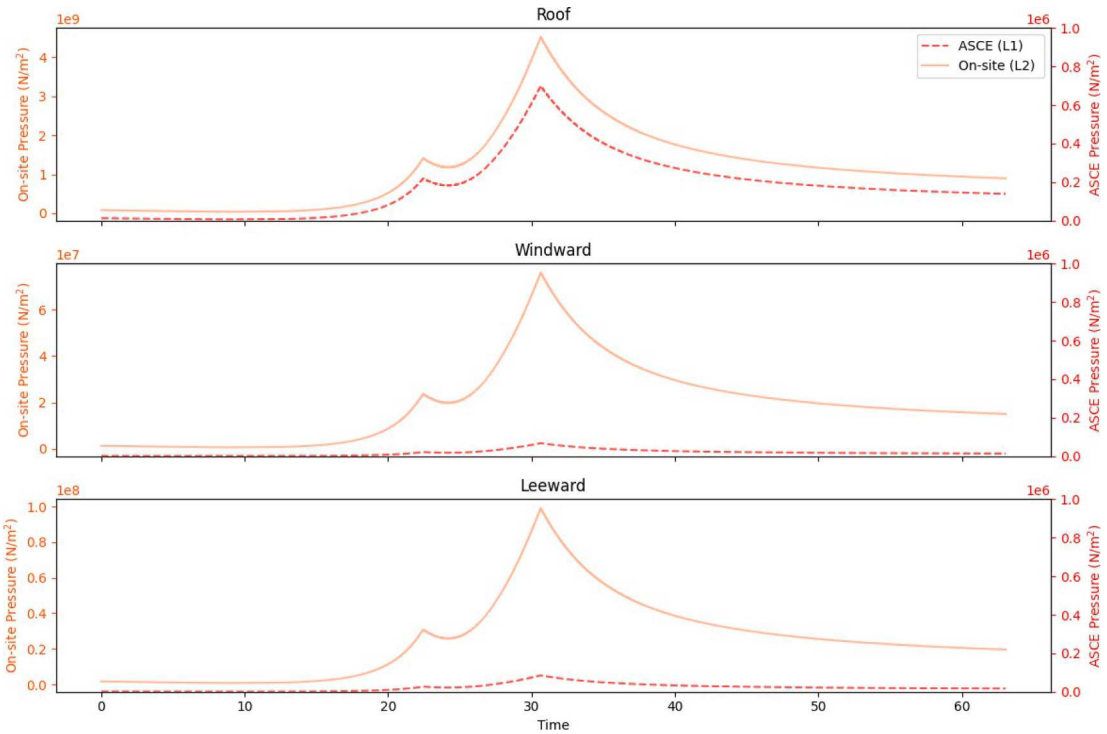

Fig. 10. The pressure variations when subjected to ASCE (L1) and On-site (L2) loading conditions.

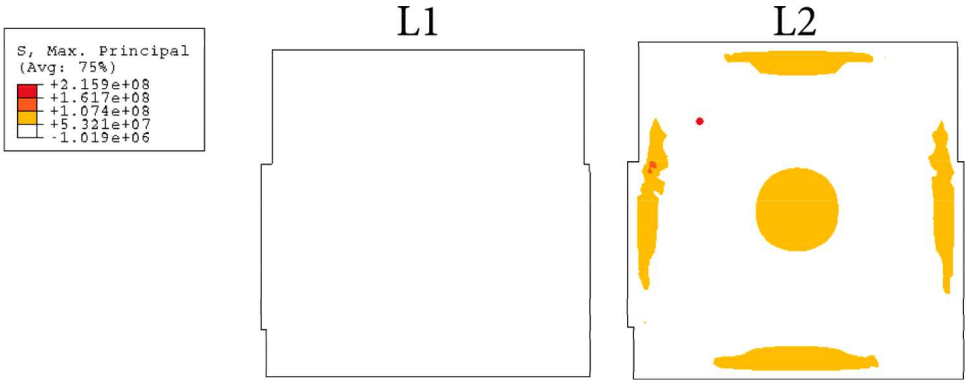

(a) The different principal stresses generated by the two loading conditions on the roof

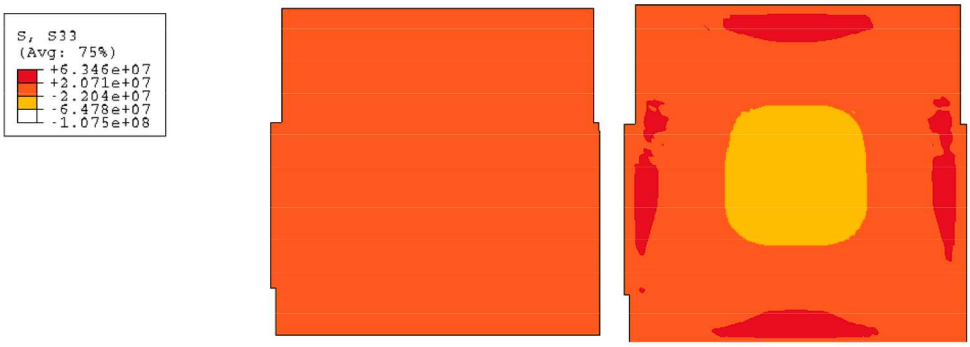

(b) The different uplift forces generated by the two loading conditions on the roof

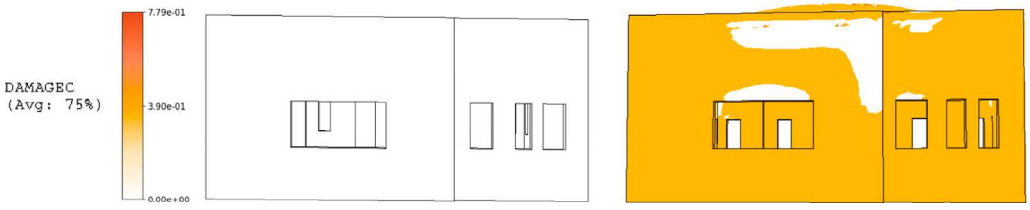

(c) Compressive stresses generated by the two loading conditions on the windward wall

Fig. 11. The different stress variations when subjected to ASCE (L1) and On-site (L2) loading conditions.

resulted in significantly elevated stress levels within the primary wind force-resisting system, aligning qualitatively with the areas of impact on the structure. It is noteworthy that, irrespective of the evaluation direction, the on-site (L2) loading condition consistently yielded higher stress values. The analysis revealed notable differences in the stresses experienced by the building under on-site speeds compared to those under ASCE 7-22 standard wind speeds.

4. Discussion

As a result of the findings and revisiting the central research inquiry posed in this paper, "To what extent do the observed structural damages and stress distributions in historic masonry buildings affected by tornadoes deviate from the predictions made by the current ASCE 7-22 standard for tornado loads?", it is evident that the on-site damages and stress distributions significantly surpass those predicted by the ASCE 7-22 standard for tornado loads. This discrepancy highlights a gap in the existing standards and underscores the need for a comprehensive reevaluation of how historic masonry buildings are assessed and strengthened in tornado-prone regions. The

results suggest that the ASCE 7-22 standards, while robust for general construction, may not fully encapsulate the vulnerabilities and structural behaviors of historic masonry buildings under extreme wind loads.

Given this, while exploring the implications these results have on the assessment, strengthening, and preservation of historic structures, the authors advocate for the development of more nuanced, preservation-compatible guidelines that can better predict and mitigate the risks to these structures. Guidelines such as these, would not only need to integrate structural analysis techniques but also respect the architectural integrity and historical value of the buildings in question. Preserving heritage in tornado-prone regions requires implementing strategic reinforcement techniques, tie-down systems, and load path strengthening without compromising the historic fabric. By investigating how historic structures and tornado impact is similar and different from ASCE 7-22 loading, will help in providing minimal intervention and maximizing the resilience of these structures. Developing such strategies necessitates a multi-disciplinary approach, integrating insights from structural engineering, material science, historic preservation, and computational modeling.

The limitation of this study lies in its focus solely on the Post Office, and the simplified numerical simulations conducted to comprehend the overall behavior and compare stress concentrations for on-site versus ASCE wind speeds. On comparing the behaviour of other masonry structures in Mayfield, it was observed that they all underwent similar damage (Fig. 12). The increased roof pressures caused uplift, subsequently destabilizing lateral support and causing wall collapses. Given that these load-bearing walls typically lack internal reinforcement, they are also vulnerable to disintegration and expulsion resulting from tornado-induced pressures.

Furthermore, this behavior is not isolated to this specific tornado event. Both the EF5 tornado that struck Joplin, Missouri in 2011 and the EF3 tornado that hit Nashville, Tennessee in 2020 had similar impacts on masonry structures. In the aftermath of the Joplin tornado, masonry structures exhibited damage along horizontal lines, where failure of load-bearing walls resulted in either partial or total roof collapse [47]. Similarly, during the Nashville tornado, intense winds caused masonry walls to fail, resulting in partial or complete roof collapses [44]. During a tornadic event, the breach in doors or windows causes a rapid increase in internal pressure leading to uplift of the roof or wall collapses originating due to weak connections [45]. These failures highlight the critical importance of continuous tie elements and properly anchored roof diaphragms in masonry construction to withstand the powerful uplift forces and internal pressures created by tornado wind loads. Many of these masonry buildings lacked the structural enhancements necessary to transfer the induced tornado loads through an intact load path. Thus, these consistent failure patterns observed in masonry structures across different tornado events emphasize the urgent need for improved building standards, specifically for older constructions and retrofitting measures to enhance their resilience against extreme wind forces.

5. Conclusion

Tornadoes have long presented a formidable challenge to the built environment, especially in the United States, where nearly a thousand tornadoes occur annually. Despite their sporadic yet devastating nature, it's only in recent years that the ASCE 7-22 standard has incorporated tornado loading considerations, primarily for structures falling under Risk Category III and IV. While previous research has extensively examined the behavior of wooden or residential structures under tornado conditions, masonry structures, often found in historic districts, have been overlooked.

During post-tornado reconnaissance, these historic masonry structures, typically designated as Risk Category II, have sustained substantial damage. This study aims to assess their performance and compare the stress distributions encountered on-site with those prescribed by design standards. To achieve this, the research utilizes simulations of a structure impacted during the December 2021 Midwest Tornado. Based on the research findings and the central research inquiry posed in this paper, it is clear that the structural damages and stress distributions observed in historic masonry buildings affected by tornadoes surpass the predictions outlined in the ASCE 7-22 standard for tornado loads, irrespective of their assumed Risk Category. This disparity highlights a deficiency in existing standards and emphasizes the necessity for a thorough reassessment of how historic masonry buildings are evaluated and fortified in

(a) American Legion **(b)** Urban Outfitters

Fig. 12. Masonry buildings in Mayfield showcasing similar damages.

tornado-prone areas.

Consequently, there is a pressing need for the development of more nuanced, preservation-compatible guidelines that can better predict and mitigate the risks to these structures. Such guidelines must integrate structural analysis techniques while respecting the architectural integrity and historical significance of the buildings. By understanding how historic structures respond to tornadoes, as compared to the ASCE 7-22 loads, will allow for minimal intervention strategies to enhance the resilience of these structures. This necessitates a multidisciplinary approach, integrating insights from structural engineering, material science, historic preservation, and computational modeling.

Furthermore, while this study primarily focuses on the US Post Office, the observed behavior of other masonry structures in Mayfield reinforces the necessity for targeted preservation strategies addressing common damage patterns and vulnerabilities across historic districts. In conclusion, this research opens avenues of discussion pertaining to the decision-making and proactive measures to safeguard cultural heritage in the face of tornado events.

CRediT authorship contribution statement

Saanchi S. Kaushal: Writing – original draft, Software, Methodology, Investigation, Formal analysis, Data curation, Conceptualization. **Mariantonieta Gutierrez Soto:** Writing – review & editing, Supervision, Conceptualization. **Rebecca Napolitano:** Writing – review & editing, Supervision, Conceptualization.

Declaration of competing interest

The authors declare the following financial interests/personal relationships which may be considered as potential competing interests: [Rebecca Napolitano reports financial support was provided by National Science Foundation. If there are other authors, they declare that they have no known competing financial interests or personal relationships that could have appeared to influence the work reported in this paper].

Data availability

Data will be made available on request.

Acknowledgements

This material is based upon work supported by the National Science Foundation under Grant No.IIS-2123343 and CMMI-2222849. Any opinions, findings, and conclusions, or recommendations expressed in this material do not necessarily reflect the views of the National Science Foundation. The authors would like to thank Professor Frank Lombardo and Daniel Rhee for sharing their wind speed estimations for Mayfield, KY. This material was also supported by Keely Patelski, Texas Tech University. The larger team that helped collect the data were graduate students from Penn State University including Daniele Melo Santos Paulino, Muhammad Rakeh Saleem, Mina Savaroliya, Alejandro Palacio Bentacur and David Eduardo Caballero Russi, and Professor Thomas Boothby. The authors acknowledge the data collection by undergraduate student Garrett Demaree from the University of Kentucky. The authors also acknowledge the members of the RAPID team from the University of Washington who helped collect and process the data.

References

[1] Asce hazard tool. https://ascehazardtool.org. Accessed: December 10, 2023.
[2] ABAQUS. ABAQUS. *Dassault Systemes Simulia Corporation, Providence, RI, USA*, page 3, 2022.
[3] M. Acito, M. Bocciarelli, C. Chesi, G. Milani, Collapse of the clock tower in finale emilia after the emilia romagna earthquake sequence: Numerical insight, Eng. Struct. 72 (70–91) (2012) 2014.
[4] Q. Albu-Jasim, Z. Medina-Cetina, A. Muliana, Calibration of a concrete damage plasticity model used to simulate the material components of unreinforced masonry reinforced concrete infill frames, Mater. Struct. 55 (2) (2022) 36.
[5] American Society of Civil Engineers. *Minimum Design Loads and Associated Criteria for Buildings and Other Structures*. American Society of Civil Engineers, asce/sei 7-22 edition, 2022.
[6] E.P. Baltsavias, A comparison between photogrammetry and laser scanning, ISPRS J. Photogrammetry Remote Sensing 54 (2–3) (1999) 83–94.
[7] A. Barbasiewicz, T. Widerski, K. Daliga, The analysis of the accuracy of spatial models using photogrammetric software: agisoft photoscan and pix4d, in: E3S Web of Conferences, 26, EDP Sciences, 2018, p. 00012.
[8] S. Gonizzi Barsanti, G. Guidi, A new methodology for the structural analysis of 3d digitized cultural heritage through fea, in: IOP Conference Series: Materials Science and Engineering, 364, IOP Publishing, 2018, p. 012005.
[9] M. Bassier, G. Hardy, L. Bejarano-Urrego, A. Drougkas, E. Verstrynge, K. Van Balen, M. Vergauwen, Semi-automated creation of accurate fe meshes of heritage masonry walls from point cloud data, in: Structural Analysis of Historical Constructions: an Interdisciplinary Approach, Springer, 2019, pp. 305–314.
[10] V. Beck, N. Dotzek, Reconstruction of near-surface tornado wind fields from forest damage, J. Appl. Meteorol. Climatology 49 (7) (2010) 1517–1537.
[11] Andrea Biasion, T Moerwald, Bernd Walser, and G Walsh. A new approach to the terrestrial laser scanner workflow: the rtc360 solution. *FIG Working Week 2019: Geospatial Information for a Smarter Life and Environmental Resilience*, 2019.
[12] A. Borri, M. Corradi, G. Castori, A. De Maria, A method for the analysis and classification of historic masonry, Bull. Earthquake Eng. 13 (2015) 2647–2665.
[13] Geoffrey Neville Boughton. *Tropical cyclone Yasi: Structural damage to buildings*. James Cook University, 2012.
[14] H.E. Brooks, G.W. Carbin, P.T. Marsh, Increased variability of tornado occurrence in the United States, Science 346 (6207) (2014) 349–352.
[15] A. Carpinteri, S. Invernizzi, G. Lacidogna, In situ damage assessment and nonlinear modelling of a historical masonry tower, Eng. Struct. 27 (3) (2005) 387–395.
[16] J. Case, P. Sarkar, S. Sritharan, Effect of low-rise building geometry on tornado-induced loads, J. Wind Eng. Indust. Aerodynamics 133 (2014) 124–134.

[17] G. Castellazzi, A.M. D'Altri, S. de Miranda, F. Ubertini, An innovative numerical modeling strategy for the structural analysis of historical monumental buildings, Eng. Struct. 132 (2017) 229–248.
[18] G. Castellazzi, N.L. Presti, A.M. D'Altri, S. de Miranda, Cloud2fem: A finite element mesh generator based on point clouds of existing/historical structures, SoftwareX 18 (2022) 101099.
[19] The case of india, Thainswemong Choudhury, Gabriele Milani, and Hemant B Kaushik. Comprehensive numerical approaches for the design and safety assessment of masonry buildings retrofitted with steel bands in developing countries, Construct. Build. Mater. 85 (2015) 227–246.
[20] E. Cuadros-Rojas, S. Saloustros, N. Tarque, L. Pelà, Photogrammetry-aided numerical seismic assessment of historical structures composed of adobe, stone and brick masonry. application to the san juan bautista church built on the inca temple of huaytará, peru, Eng. Fail. Anal. 158 (2024) 107984.
[21] S. de Antonio Maria D'Altri, G.C. Miranda, B. Glisic, Numerical modelling-based damage diagnostics in cultural heritage structures, J. Cultural Heritage 61 (2023) 1–12.
[22] S.D. Abbati, A.M. D'Altri, D. Ottonelli, G. Castellazzi, S. Cattari, S. de Miranda, S. Lagomarsino, Seismic assessment of interacting structural units in complex historic masonry constructions by nonlinear static analyses, Comput. Struct. 213 (2019) 51–71.
[23] A.M. D'Altri, V. Sarhosis, G. Milani, J. Rots, S. Cattari, S. Lagomarsino, E. Sacco, A. Tralli, G. Castellazzi, S. de Miranda, Modeling strategies for the computational analysis of unreinforced masonry structures: review and classification, *Arch. Comput. Methods Eng.* 27 (2020) 1153–1185.
[24] SM. Motovali Emami, M. Mohammadi, Influence of vertical load on in-plane behavior of masonry infilled steel frames, Earthquakes and Structures 11 (4) (2016) 609–627.
[25] A. Finch, Death Toll Climbs from One of the Costliest Tornado Events in History 10 (2022) 2021.
[26] F.L. Haan Jr, V.K. Balaramudu, P.P. Sarkar, Tornado-induced wind loads on a low-rise building, J. Struct. Eng., ASCE 136 (1) (2010) 106–116.
[27] F.L. Haan Jr, P.P. Sarkar, W.A. Gallus, Design, construction and performance of a large tornado simulator for wind engineering applications, Eng. Struct. 30 (4) (2008) 1146–1159.
[28] T. Hinks, H. Carr, L. Truong-Hong, D.F. Laefer, Point cloud data conversion into solid models via point-based voxelization, J. Surveying Eng. 139 (2) (2013) 72–83.
[29] John Dean Holmes. *Wind loads on low rise buildings: A review*. Commonwealth Scientific and Industrial Research Organization, Division of Building Research, 1983.
[30] R. Honerkamp, G. Yan, D. Han, R. Feng, Z. Li, T. Li, Tornado-induced structural damage based on reconnaissance surveys of the 2019 jefferson city, missouri, tornado and previous notable tornadoes, Nat. Hazards. Rev. 23 (4) (2022) 05022008.
[31] Hu. Hui, Z. Yang, P. Sarkar, F. Haan, Characterization of the wind loads and flow fields around a gable-roof building model in tornado-like winds, Experiments in Fluids 51 (3) (2011) 835–851.
[32] Nicko Kassotakis, Vasilis Sarhosis, Belen Riveiro, Borja Conde, Antonio Maria D'Altri, Jon Mills, Gabriele Milani, Stefano de Miranda, and Giovanni Castellazzi. Three-dimensional discrete element modelling of rubble masonry structures from dense point clouds. *Automation in Construction*, 119:103365, 2020.
[33] Saanchi S Kaushal, Mariantonieta Gutierrez Soto, and Rebecca Napolitano. 3D Digital Documentation of Tornado-Damaged Heritage Buildings. *Journal of Structural Engineering*, 2024. Accepted for publication.
[34] A. Kita, N. Cavalagli, M.G. Masciotta, P.B. Lourenço, F. Ubertini, Rapid post-earthquake damage localization and quantification in masonry structures through multidimensional non-linear seismic ida, Eng. Struct. 219 (2020) 110841.
[35] Gregory A Kopp. Large-scale and full-scale laboratory test methods for examining wind effects on buildings, 2018.
[36] Y. Li, L. Zhao, Y. Chen, Na. Zhang, H. Fan, Z. Zhang, 3d lidar and multi-technology collaboration for preservation of built heritage in china: a review, Int. J. Appl. Earth Observation Geoinformation 116 (2023) 103156.
[37] Z. Liu, T. Ishihara, A study of tornado induced mean aerodynamic forces on a gable-roofed building by the large eddy simulations, J. Wind Eng. Indust. Aerodynamics 146 (2015) 39–50.
[38] Z. Liu, C. Zhang, T. Ishihara, Numerical study of the wind loads on a cooling tower by a stationary tornado-like vortex through les, J. Fluids Struct. 81 (2018) 656–672.
[39] Franklin T. Lombardo, Engineering analysis of a full-scale high-esolution tornado wind speed record, *J. Struct. Eng.* 144 (2) (2018) 04017212.
[40] F.T. Lombardo, D.B. Roueche, D.O. Prevatt, Comparison of two methods of near-surface wind speed estimation in the 22 may, joplin, missouri tornado, J. Wind Eng. Indust. Aerodynamics 138 (87–97) (2011) 2015.
[41] Jacob Lubliner, Javier Oliver, Sand Oller, EJIJos Onate, A plastic damage model for concrete, *Int. J. Solids Struct.* 25 (3) (1989).
[42] T. Maloney, B. Ellingwood, H. Mahmoud, N. Wang, Y. Wang, P. Lin, Performance and risk to light-framed wood residential buildings subjected to tornadoes, Struct. Safety 70 (2018) 35–47.
[43] Tim Marshall, Scott Morrison, and Jeffrey Green Haag. On the performance of brick and concrete masonry in windstorms. In *25th Conference on Severe Local Storms*, Denver, CO, August 2010.
[44] Tim Marshall, Christine Standohar-Alfano, Christopher Bright, and Krissy Hurley. Damage survey of the nashville, tn tornado: March 3, 2020. In *Proceedings of the 30th Conference on Severe Local Storms*, Santa Fe, NM, November 2022.
[45] Tim Marshall, Zachary B. Wienhoff, Brian E. Smith, and Christine L. Wielgos. Damage survey of the mayfield, ky tornado: 10 december 2021. In *30th Conference on Severe Local Storms*, Santa Fe, NM, November 2022.
[46] T.P. Marshall, Tornado damage survey at moore, oklahoma, Weather and Forecasting 17 (2002).
[47] Timothy P Marshall. Performance of concrete masonry buildings in the joplin tornado. *American Meteorological Society http://ams. confex. com/ams/92Annual/webprogram/8IMPACTS. html*, 2012.
[48] J.R. McDonald, K.C. Mehta, D.A. Smith, J. Arn Womble, The enhanced fujita scale: development and implementation. in *forensic engineering 2009*, Pathol. Built. Environ. (2010) 719–728.
[49] X. Meng, N. Currit, K. Zhao, Ground filtering algorithms for airborne lidar data: a review of critical issues, Remote Sensing 2 (3) (2010) 833–860.
[50] J.E. Minor, J.R. McDonald, K.C. Mehta, The Tornado: an Engineering-Oriented Perspective. (1993).
[51] M.J. Morrison, G.A. Kopp, E. Gavanski, C. Miller, A. Ashton, Assessment of damage to residential construction from the tornadoes in vaughan, ontario, Canadian J. Civil Eng. 41 (6) (2014) 550–558, on 20 august 2009.
[52] S.M.M. Emami, M. Mohammadi, P.B. Lourenço, Equivalent diagonal strut method for masonry walls in pinned connection and multi-bay steel frames, J. Seismol. Earthquake Eng. 19 (4) (2017) 299–311.
[53] R. Napolitano, B. Glisic, Hybrid physics-based modeling and data-driven method for diagnostics of masonry structures, Computer-Aided Civil Infrastruct. Eng. 35 (5) (2020) 483–494.
[54] National Register of Historic Places. National Register Of Historic Places Nomination Form: Mayfield Downtown, 1984. Register Number 84001477.
[55] National Register of Historic Places. National Register Of Historic Places Nomination Form: Mayfield Downtown Commercial District District Expansion, 1996. Register Number 96000791.
[56] Stephanie Pappas. Quad-state tornado may be longest-lasting ever, December 2021.
[57] S. Pilkington, D. Roueche, M. Gutierrez Soto, M. Alam, R. Napolitano, T. Kijewski-Correa, D. Prevatt, S.S. Kaushal, J. Nakayama, M. Saleem, H. Ibrahim, A. Lyda, H. Lester, D. Caballero-Russi, I. Gurley, K. Robertson, F. Lombardo, StEER: 10 december 2021 midwest tornado outbreak joint preliminary virtual reconnaissance report and early access reconnaissance report (PVRR-EARR). StEER - 10, Midwest Tornado Outbreak, DesignSafe-CI. 1 (1–15) (2021) 2021.
[58] David O Prevatt, David B Roueche, John W Van De Lindt, Shiling Pei, Thang Dao, William Coulbourne, Andrew J Graettinger, Rakesh Gupta, and David Grau. Building damage observations and ef classifications from the tuscaloosa, al, and joplin, mo, tornadoes. In *Structures Congress 2012*, pages 999–1010, 2012.
[59] J Stanley Rabun. Structural Analysis of historic buildings: Restoration, preservation, and adaptive reuse applications for Architects and Engineers. John Wiley & Sons, 2000.
[60] D.M. Rhee, M.L. Levitan, J. LaDue, Wind speed estimates of the december 2021 quad-state tornado in mayfield, ky based on treefall pattern analysis, Data Publication (2023), https://doi.org/10.18434/mds2-3025.

[61] D.M. Rhee, F.T. Lombardo, Improved near-surface wind speed characterization using damage patterns, J. Wind Eng. Indust. Aerodynamics 180 (2018) 288–297.
[62] D.M. Rhee, J.B. Nevill, F.T. Lombardo, Comparison of near-surface wind speed estimation techniques using different damage indicators from a damage survey of naplate, il ef-3 tornado, Nat. Hazard. Rev. 23 (1) (2022) 04021052.
[63] P. Roca, M. Cervera, G. Gariup, L. Pela', Structural analysis of masonry historical constructions. classical and advanced approaches, Archives Comput. Methods Eng. 17 (2010) 299–325.
[64] R. Rolin, E. Antaluca, J.-L. Batoz, F. Lamarque, M. Lejeune, From point cloud data to structural analysis through a geometrical hbim-oriented model, J. Computing Cultural Heritage (JOCCH) 12 (2) (2019) 1–26.
[65] D.B. Roueche, G. Chen, M.G. Soto, S. Kameshwar, A. Safiey, T. Do, F.T. Lombardo, J.O. Nakayama, B.M. Rittelmeyer, A. Palacio-Betancur, G. Demaree, Performance of hurricane-resistant housing during the 2022 arabi, louisiana, tornado, J. Struct. Eng. 150 (5) (2024) 04024029.
[66] Bruce Schreiner and Dylan Lovan. Kentucky tornado toll in dozens; less than feared at factory. https://apnews.com/article/tornadoes-kentucky-illinois-arkansas-tennessee-missouri-e1ae21e0b7521c28411f8c360b756700, December 2021.
[67] K.M. Simmons, D. Sutter, Improvements in tornado warnings and tornado casualties, Int. J. Mass Emergencies Disasters 24 (3) (2006) 351.
[68] P.R. Sparks, H. Liu, H.S. Saffir, Wind damage to masonry buildings, J. Aerospace Eng. 2 (4) (1989) 186–198.
[69] C.D. Standohar-Alfano, J.W. van de Lindt, Tornado risk analysis for residential wood-frame roof damage across the united states, J. Struct. Eng. 142 (1) (2016) 04015099.
[70] T. Stathopoulos, H. Alrawashdeh, Wind loads on buildings: a code of practice perspective, J. Wind Eng. Indust. Aerodynamics 206 (2020) 104338.
[71] S.A. Stevenson, A.M. El Ansary, G.A. Kopp, A practical modelling technique to assess the performance of wood-frame roofs under extreme wind loads, Eng. Struct. 191 (2019) 640–648.
[72] H. Thampi, V. Dayal, P.P. Sarkar, Finite element analysis of interaction of tornados with a low-rise timber building, J. Wind Eng. Indust. Aerodynamics 99 (4) (2011) 369–377.
[73] Lawrence Twisdale, Sudhan Banik, Lauren Mudd, Marshall Hardy, Shahriar Quayyum, Fangqian Liu, Melissa Faletra, Peter Vickery, Marc Levitan, and Long Phan. Tornado wind speed maps for building design: Research and development of tornado risk assessment methodology, 2023-10-02 04:10:00 2023.
[74] M. Valente, G. Milani, Seismic assessment of historical masonry towers by means of simplified approaches and standard fem, Construct. Build. Mater. 108 (2016) 74–104.
[75] J. Wang, S. Cao, Characteristics of tornado wind loads and examinations of tornado wind load provisions in asce 7–16, Eng. Struct. 241 (2021) 112451.
[76] R. Wood, D. Roueche, K. Cullum, B. Davis, M. Gutierrez Soto, S. Javadinasab Hormozabad, Y. Liao, F. Lombardo, M. Moravej, S. Pilkington, D. Prevatt, T. Kijewski-Correa, W. DJIMA, and I. Robertson. Early Access Reconnaissance Report (EARR). DesignSafe-CI, 2020. StEER - 3 March 2020 Nashville Tornadoes.
[77] Wu. Chao, Y. Yuan, Y. Tang, B. Tian, Application of terrestrial laser scanning (tls) in the architecture, engineering and construction (aec) industry, Sensors 22 (1) (2021) 265.
[78] Xu. Feng, J. Ma, W.-l. Chen, Y.-Q. Xiao, Z.-D. Duan, Analysis of load characteristics and responses of low-rise building under tornado, Procedia Eng. 210 (2017) 165–172.